Distributed Augmented Reality With 3-D Lung Dynamics—A Planning Tool Concept

Felix G. Hamza-Lup, Anand P. Santhanam, Celina Imielińska, Sanford L. Meeks, and Jannick P. Rolland

***Abstract*—Augmented reality (AR) systems add visual information to the world by using advanced display techniques. The advances in miniaturization and reduced hardware costs make some of these systems feasible for applications in a wide set of fields. We present a potential component of the cyber infrastructure for the operating room of the future: a distributed AR-based software–hardware system that allows real-time visualization of three-dimensional (3-D) lung dynamics superimposed directly on the patient's body. Several emergency events (e.g., closed and tension pneumothorax) and surgical procedures related to lung (e.g., lung transplantation, lung volume reduction surgery, surgical treatment of lung infections, lung cancer surgery) could benefit from the proposed prototype.**

***Index Terms*—Augmented reality (AR), deformable three-dimensional (3-D) models, distributed systems, 3-D simulation, virtual reality.**

I. Introduction

Augmented reality (AR) allows the development of promising tools in several domains, from design and manufacturing [1] to medical applications [2], [3]. We present a potential component of the cyber infrastructure for the operating room of the future: a distributed AR-based software–hardware system that allows real-time visualization of three-dimensional (3-D) lung dynamics superimposed directly on the patient's body. The application domain for the proposed cyber infrastructure includes training students on clinical procedures (e.g., intubation) and planning clinical interventions. Specifically, pre-, intra-, and postoperative assessments for emergency events (e.g., closed and tension pneumothorax), and pre- and postoperative assessments for surgical procedures related to the lung (e.g., lung transplantation, lung volume reduction surgery, surgical treatment of lung infections, and lung cancer surgery) could benefit from the proposed visualization tool. The tool also facilitates experts' interactions, especially during quick-response conditions, such as medical emergencies in geographically inaccessible locations [4]. In this paper, an AR-based visualization system is integrated with a human patient simulator (HPS). The integrated prototype provides a simulation and training test-bed that most closely resembles the clinical-end application.

This paper exemplifies advanced medical visualization paradigms, where known methodologies in different technical fields are combined and tailored to best serve the requirements of the application. Specifically, we use the methods discussed in [5] and [6] to model the real-time 3-D lung dynamics and biomathematics, respectively.

An early integration of the real-time 3-D lung dynamics with a distributed AR-based framework was presented in [7], where the real-time 3-D lung dynamics were superimposed on the HPS. In this earlier integration, we demonstrated the possibility for remotely located clinical technicians to view the 3-D lung dynamics of a patient in real time. We extend our previous work by concentrating on the integration of the hardware and software for the development of a prototype that could be a part of the operating rooms in the near future.

The paper is structured as follows. Section II presents the AR planning tool concept followed by the related work on modeling 3-D lung dynamics in Section III. Section IV summarizes the hardware components involved. Modeling 3-D lung dynamics and the data distribution scheme are presented in Section V. Results and preliminary assessments are detailed in Section VI, followed by discussions, conclusions, and future work in Sections VII and VIII.

II. Planning Tool Concept

The distributed interactive tool aimed at surgical planning allows visualization of virtual 3-D deformable lung models overlaid on the patient's body in an effort to improve the medical planning process.

The planner and other medical personnel, located remotely, may be involved in the surgical planning procedure and may visualize the 3-D lung model while seeing and interacting with each other in a natural way [Fig. 1(a)]. Moreover, they are able to participate in the planning procedure by pointing and drawing diagrams corresponding to the 3-D lung model. Fig. 1(b) shows the superimposition concept: the virtual 3-D model of the lung overlaid on the patient's thoracic cage.

The remote medical personnel interacting with the (local) planner can see the changes in the lung behavior and will adopt different planning choices. Such an advanced planning tool has the potential to:

Manuscript received September 30, 2005; revised April 17, 2006. This work was supported in part by the Link Foundation, in part by the Florida Photonics Center of Excellence, in part by the U.S. Army STRICOM, and in part by NVIS, Inc.

F. G. Hamza-Lup is with the School of Computing, Armstrong Atlantic State University, Savannah, GA 31419 USA (e-mail: felix@cs.armstrong.edu).

A. P. Santhanam is with the School of Computer Science, University of Central Florida (UCF), Orlando, FL 32816-2993 USA.

C. Imielińska is with the Department of Medical Informatics, College of Physicians and Surgeons, and also with the Department of Computer Science, Columbia University, New York, NY 10032 USA (e-mail: cei7001@dbmi.columbia.edu).

S. L. Meeks is with the Department of Radiation Physics, M.D. Anderson Cancer Center, Orlando, FL 32806 USA.

J. P. Rolland is with the Department of Optics, College of Optics and Photonics, University of Central Florida (UCF), Orlando, FL 32816 USA.

Digital Object Identifier 10.1109/TITB.2006.880552

(a) (b)

Fig. 1. (a) Surgical planning personnel interacting with 3-D models. (b) User's view of the virtual 3-D model of the lungs as he/she interacts with the participants in (a).

1) involve local and remote planning personnel in the surgical planning procedure, opening new ways of collaboration and interaction;
2) enable the local planner to actually "see" the anatomical model (patient-specific data) superimposed on the patient and, therefore, improve the surgical plan.

III. Related Work

With these concepts in mind, we provide a brief review of the techniques and algorithms that support the rendering of the dynamic 3-D lung models, as well as an important issue in distributed simulations, the dynamic shared state.

A. Deformable Lung Models

Early attempts to model lung deformation were based on the lung physiology and clinical measurements [8]. The physical deformation of lungs, as a linearized model, was proposed by Promayon [9], followed by a finite element model (FEM) based deformation for modeling pneumothorax-like conditions [10]. An early functional FEM model for the lung tissue constituents (i.e., parenchyma, bronchiole, and alveoli) of lungs aimed at analyzing the anatomical functions of the lung during breathing [11]. The computational complexity of the approach was reduced by modeling only the bronchioles and the airflow inside them [12].

Nonphysical methods for lung deformation combined nonuniform rational B-spline surfaces based on data from patients' computed tomography scans [13].

B. Distributed Interactive Simulations

In distributed interactive simulations, the interactions and information exchange generate a state referred to as the *dynamic shared state*, which has to remain consistent for all participants at all sites. The interactive and dynamic nature of a distributed simulation is constrained by the communication latency, as well as by the complex visualization and rendering systems latencies.

A number of consistency maintenance techniques have been employed in the distributed environments and the research efforts can be grouped in four categories: communication protocol optimization, virtual space management, human perceptual limitation [14], and system architecture [15].

AR systems were proposed in the mid-1990s as tools to assist different fields: medicine [16], complex assembly labeling [17], and construction labeling [18]. With advances in computer graphics, tracking systems, and 3-D displays, the research community has shifted attention to distributed collaborative environments that extensively use the AR paradigm [19].

(a) (b)

Fig. 2. Collections of LED (i.e., tracking probes). (a) Optical see-through HMD developed through an interdisciplinary research effort at ODALab, University of Central Florida (courtesy NVIS, Inc., for the opto-mechanical design) and custom-designed semispherical head-tracking probe. (b) Patient-tracking probe.

IV. Hardware Components

Our system integrates a 3-D visualization device with an optical tracking system and a Linux-based PC. With the exception of the 3-D visualization device, the prototype was integrated using commercially available hardware components.

A. Visualization Device

To see the 3-D model, the planner and the other users wear lightweight head-mounted displays (HMDs) [Fig. 2(a)] [20].

A key component in the reduction of weight in the optical design for HMD is the optimal integration of diffractive and plastic optics as well as various emerging optical materials that may be used to compensate for the optical aberrations responsible for image degradation. Optics as light as six grams per eye have been achieved for horizontal field of views as large as 70°. The current projection resolution of the HMD is 600×800 pixels.

B. Tracking System

To superimpose the 3-D virtual models at the correct location with respect to the patient, we need to track, in real-time, the relative position of the visualization device or planner's head and the patient's thoracic cage [21].

The pose (i.e., position/orientation) of the planner's head and the patient's thoracic cage are determined using an optical tracking system (i.e., Polaris Northern Digital) and two custom-built tracking probes [22], as illustrated in Fig. 2(a) and (b).

A key step in the accurate registration of the virtual lungs over the patient is the calibration procedure. In this step, the patient is positioned in the intubation posture. Magnetic resonance imaging (MRI) data of the relative position of the mandible, selected landmarks with respect to the larynx, trachea, and clavicle are collected in this posture. The inclusion of the mandible, larynx, and trachea in the previous step allows us to track the position of the intubation tube (through the mouth and upper airway) for medical procedures that require such support. The lung can be registered based on the mandible and the upper chest landmarks (e.g., clavicle). From that point on, the lungs are kept in registration with the patient, based on the location of the upper chest landmarks, together with the position of the user.

The tracking system is based on two tracking probes: one on the HMD to determine the planner's head position and orientation, and the other on the chin of the HPS to determine its location. The tracking data obtained is currently updated at 40 Hz. The tracking working volume is a cone having a height of 1.5 m and a base radius of 0.5 m.

To superimpose the 3-D virtual model of the lung on the patient, we used the least-squares pose estimation algorithm detailed in [23]. The predefined set of markers on the head-tracking probe are uniformly distributed on a hemisphere to enable 360° tracking while the user tilts his/her head.

V. Software Components

In this section, we detail the 3-D lung dynamics modeling approach and the data distribution scheme.

A. Deformable Lung Model

The virtual 3-D deformable lung model contains two components. For the first component, we parameterized the pressure–volume (*PV*), i.e., the relation between the lung volume and the trans-pulmonary pressure [24]. The relation represented as a set of control constants and basis functions allowed us to model subject-specific breathing patterns and their variations. Variations in breathing may be caused by abnormalities, such as pneumothorax, tumors, or dyspnea. These variations lead to changes in the *PV* curve of the patient and can be modeled by the controlled modulations of the basis functions and control constants.

For the second component, we estimated the deformation kernel of a patient-specific 3-D lung model extracted from four-dimensional (4-D) high-resolution computed tomography (HRCT). This component has been previously discussed in detail for the normal lungs [25] and tumor-influenced lungs [26]. We used Green's function (GF) based deformation for modeling the lung dynamics. The GF was represented as a convolution of the force applied on each node of the 3-D lung model and the deformation operator. The force applied on each node represented the airflow and was based on the distance from the resting surface (due to gravity). For mathematical analysis, the GF was represented in a continuous domain. The displacement of every node was computed from subject-specific 4-D HRCT and the force applied on each node was estimated for the supine position. A polar coordinate representation was used to represent each node in Green's formulation. We expanded the component functions (i.e., applied force, deformation, and the deformation operator) using spherical harmonic (SH) transformations [27]. The SH coefficients of the deformation were expressed as a direct product of the SH coefficients of the applied force and the SH coefficients of the deformation operator's row. Using this framework, the deformable 3-D lung model was implemented in OpenGL (as illustrated in Fig. 3).

A key aspect of using a physical and physiology-based model is that the resulting 3-D deformation accounts for changes in the patient's orientation, as well as in the movement of the diaphragm. The changes in the position of the diaphragm were modeled using the SH coefficients to closely simulate the effects of the diaphragm movement.

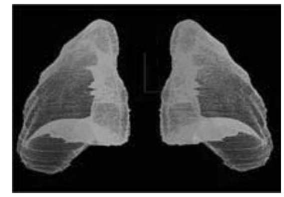

Fig. 3. High-resolution 3-D deformable lung model [28].

B. Data Distribution Scheme

To control the 3-D lung dynamics remotely, we investigated several alternatives [7]. We decided to use a bandwidth-conserving method, i.e., we aim at reducing the number of packets sent between the nodes by sending the deformation parameters as a single packet at the start of every breathing cycle. The components of this packet are the input parameters for the lung deformation which relate the intra-pleural pressure and the lung volume during breathing. Additionally, the force applied on each vertex and its elastic properties are also transmitted.

Data is distributed in the form of custom-defined data packages denoted as control packet objects (CPOs). Each packet contains the boundary values of the pressure and volume, control constants, force coefficients, and elasticity coefficients.

The boundary values for volume are the lung functional residual capacity (FRC) and tidal volume (TV). The control constants represent the PV relationship required for modeling patient's breathing condition as discussed in the first stage of 3-D lung dynamics [6]. N denotes the number of control constants. The force coefficients are the SH coefficients that describe the force applied on every node of the 3-D model. The elasticity coefficients describe the 3-D lung model's elasticity. The deformation of the 3-D model at any remote location is computed as the product between the force and elasticity coefficients.

To compensate for the communication latency, we combined the distributed application with an adaptive delay measurement algorithm [29] that estimates the delay between each pair of users and predicts the next CPO values. Fig. 4 illustrates the distribution scheme layers.

We optimized the data distribution by reducing the number of packets, i.e., for each change in the lung dynamic parameters, a CPO packet was sent. Once the packet is received, each participating node knows how to drive its own lung deformation simulation.

VI. Result and Preliminary Assessment

We have deployed the prototype using Linux-based PCs with NVidia *GeForce4* graphical processing units on our 100 Mbps local area network using a typical client–server architecture (i.e., the PC connected to the HMD was acting as the server, while other PCs, the clients, on the same network could visualize the

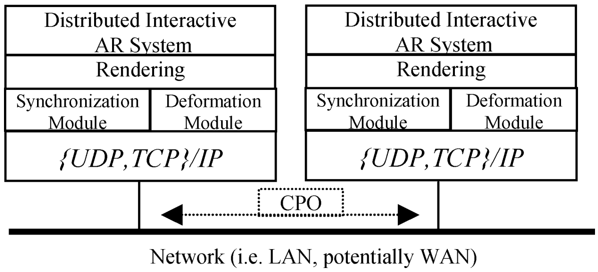

Fig. 4. Application stack layers.

(a) (b)

Fig. 5. (a) System components. (b) User's view (augmented) captured with a camera placed behind one eye in the HMD.

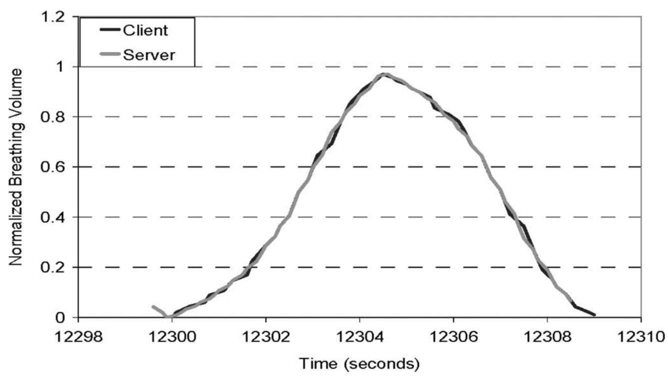

Fig. 6. 3-D lung model volume as seen on the client and server during one breathing cycle.

3-D model of the lung remotely). Instead of a real patient, we used an HPS from Medical Educational Technologies.

We superimposed the deformable model on the HPS using a Polaris infrared optical tracking system. The update cycle is combined with the deformation rendering cycle to obtain an average frame rate of 25 frames/s. Fig. 5(b) shows a camera view of the superimposition of the deformable 3-D lung model on the HPS.

A. Volume Consistency, Breathing Cycle

We obtained a smooth and synchronized view between participants, as shown by the normalized breathing volume in Fig. 6. The normalized breathing volume reached the same values over time simultaneously with each participant proving that high levels of shared state consistency can be achieved. Interactivity on such a distributed system would be consistent in terms of user's actions.

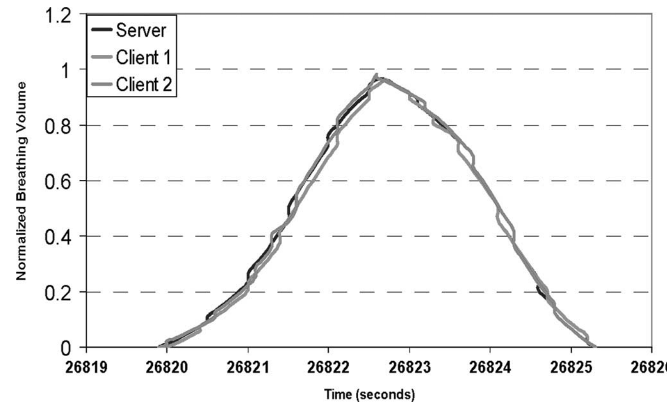

Fig. 7. 3-D lung model volume as seen by three remote collaborators during one breathing cycle.

TABLE I
HARDWARE SYSTEM ATTRIBUTES

Node no.	CPU (GHz)	RAM (GB)	GPU (GeForce)
1(server)	2.8 AMD	0.5	Ti4200
2(client)	2.4 Intel	1	Ti4800
3(client)	1.5 AMD	0.5	Ti4200

B. Preliminary Scalability Assessment

To investigate the scalability of the approach, we consecutively increased the number of participants to two and three. To quantify the scalability of the adaptive synchronization algorithm regarding the number of participants, we define a metric analyzing the relationship between the number of participants in the system and the drift values among their views.

Fig. 7 illustrates the values of the normalized breathing volume when three participants use the system. The average normalized breathing volume drift per breathing cycle was 0.01% in this case. Such small drifts in the volume values could not be subjectively observed by the users of the system. The shared state consistency ultimately depends on the network infrastructure as well as on the hardware systems complexity. The hardware attributes involved in the simulation are described in Table I.

VII. DISCUSSION

Our prototype focuses on coupling physics and physiology-based subject-specific 3-D deformable lung models with distributed AR-based visualization. The 3-D deformable models, being generated from 4-D HRCT imaging, show the effective role that such advanced systems can play in deciding clinical interventions for a wide range of disease states. Coupled with the distributed AR-based visualization, such deformable models facilitate the prototype to have user-specific views of subject-specific lungs.

From the clinical usage perspective, the prototype can be considered for training and planning under three conditions: 1) without any invasive intervention; 2) with minimal invasive intervention; and 3) with thorough invasive intervention.

1) *Without any invasive intervention*: Such clinical scenarios would include investigating a patient's general breathing

patterns and discomfort (e.g., dyspnea). For this case, the prototype allows the user to view subject-specific breathing patterns under different physical conditions and orientations of the patient.

2) *With minimal invasive intervention*: Such interventions would include procedures such as intubation, endoscope, and needle insertion, etc. During such interventions, the proposed AR prototype could be an effective tool since it can show the position of the minimally invasive tools as well as the breathing changes that are caused by the subjective discomfort and the effect of the clinical intervention.
3) *With thorough invasive intervention*: Such interventions would include preplanned procedures, such as lung transplants and lung volume reduction. Under such interventions, AR would be an effective tool for visualizing the preoperative conditions and postoperative prognosis for the patient. For instance, in the case of lung transplants, care needs to be taken regarding the changes in the subject's breathing pattern caused by: 1) pleural space complications such as pneumothorax; 2) parenchymal space complications, such as empyema; and 3) opportunistic infections such as pneumonitis. Such complications may be avoided by visualizing the patient's breathing morphology in an AR-based environment. Simulating intraoperative conditions would heavily rely on the bio-mathematical interactive 3-D models that can accurately account for user-induced variations in the subject's anatomy. For a subject-specific lung, developing such 3-D models is currently an open research problem.

We are currently in collaboration with the Department of Radiation Oncology at M.D. Anderson Cancer Center for optimizing the prototype for tracking tumor motion and morphological changes during high-precision radiation therapy.

The key technical issue that pertains to the applicability of such a prototype deals with the choice of equipment and motion compensation approach. One may note that different tracking systems may be employed along with the AR. Of particular importance is the electromagnetic tracking, which is widely used for AR applications. However, care needs to be taken on its usage since the interference between the tracking system and the surgical (metal and carbon fibers) tools present in the room can induce errors in the tracking process. Recently, micro-trackers (approximately 1 mm in diameter) have opened the use of magnetic trackers in the surgical room.

From an image perspective, the respiratory motion compensation deals with image blur caused by the imaging system. Since we extract the 3-D models using a 4-D HRCT imaging system (with breath-hold maneuver), the effect of the image blur in the 3-D models is negligible. From an image-streaming perspective, motion compensation issues are generally dealt with during image encoding and transmission over a network. However, such image-streaming approach cannot be used in a distributed AR environment as users at two different locations will have two different views of the 3-D lungs. We have, thus, eliminated the image-streaming steps by replacing them with a data distribution scheme that can synchronize the individual views of a group, as the simulation runs on different computers connected through the network.

From a simulation and visualization perspective, the respiratory motion compensation refers to nonsmooth simulations and can be considered under the following conditions:

1) *Respiratory motion compensation without patient's motion and breathing changes:* In [5], we have presented a detailed account of the respiratory motion and the generation of real-time physically based 3-D deformable lung models. A key aspect of the 3-D lung deformations is their ability to satisfy real-time constraints. Using the state-of-the-art graphics processing units, we display the lung deformation at 75 frames/s (without tracking).
2) *Respiratory motion compensation with patient's breathing variations:* In recent work, we have investigated changes in the lung dynamics of the patient, caused by the lung tissue degenerations [26], and behavioral conditions, caused by the subjective perception of the discomfort [30]. The tissue degenerations were accounted for by modifying the deformation kernel, and the subjective perception of the discomfort was simulated by modifying the pressure–volume curve.
3) *Respiratory motion compensation with patient's motion:* One may note that the task of simulating respiratory motion with the patient's motion-compensation is a complex task. In our approach, we have compensated for the patient's motion by modifying the SH coefficients of the applied force by interpolating among a set of precomputed applied forces for each orientation of the subject. The interpolation did not induce any computational delay and did not affect the real-time behavior of the simulation.

VIII. Conclusion

We have presented the integration of a distributed interactive planning prototype that enables visualization of a deformable 3-D lung model. The distribution of the deformable 3-D models at remote locations allows efficient communication of concepts, and generates a vast potential for collaboration and training.

An important assumption in the experiments is that the distributed system is composed of fairly homogeneous nodes, i.e., nodes have approximately similar rendering and communication capabilities. The experiments were performed on a low latency network with up to three nodes, one server and two clients. We plan to increase the number of users to further test the scalability of the prototype, and to assess the efficiency of the system from the human factors' perspective.

Future work involves adding disease states such as the chronic obstructive pulmonary disease, dyspneac breathing, and pneumothorax-influenced 3-D lung deformations.

References

[1] S. K. Ong and A. Y. C. Nee, *Virtual and Augmented Reality Applications in Manufacturing*. London, U.K.: Springer-Verlag, 2004.

[2] A. State, M. A. Livingston, G. Hirota, W. F. Garrett, M. C. Whitton, H. Fuchs, and E. D. Pisano, "Technologies for augmented-reality systems: Realizing ultrasound-guided needle biopsies," presented at the SIGGRAPH Conf., New Orleans, LA, Aug. 1996.

[3] F. G. Hamza-Lup, J. P. Rolland, and C. E. Hughes, "A distributed augmented reality system for medical training and simulation," in *Energy, Simulation-Training, Ocean Engineering and Instrumentation: Research Papers of the Link Foundation Fellows,* vol. 4, Rochester, NY: Univ. of Rochester Press, 2004, pp. 213–235.

[4] B. H. Thomas, G. Quirchmayr, and W. Piekarski, "Through-walls communication for medical emergency services," *Int. J. Human–Comput. Interact.*, vol. 16, pp. 477–496, 2003.

[5] A. Santhanam, C. Fidopiastis, F. Hamza-Lup, J. P. Rolland, and C. Imielinska, "Physically-based deformation of high-resolution 3D lung models for augmented reality based medical visualization," presented at the AMI-ARCS Conf., Rennes, France, 2004.

[6] A. Santhanam, C. Fidopiastis, A. Tal, B. Hoffman Ruddy, and J. P. Rolland, "An adaptive driver and real-time deformation algorithm for visualization of high-density lung models," *Stud. Health Technol. Inform.*, vol. 98, pp. 333–339, 2004.

[7] F. G. Hamza-Lup, A. Santhanam, C. Fidopiastis, and J. P. Rolland, "Distributed training system with high-resolution deformable virtual models," presented at the 43rd Annu. ACM Southeast Conf., Kennesaw, GA, 2005.

[8] J. R. Ligas and F. P. J. Primiano, "Respiratory mechanics," in *Encyclopedia of Medical Instrumentation*, J. G. Webster, Ed. New York: Wiley, 1988, pp. 2550–2573.

[9] E. Promayon, P. Baconnier, and C. Puech, "Physically-based model for simulating the human trunk respiration movements.," in *Proc. Int. Joint Conf. CVRMED MRCAS*, 1997, vol. 1205, pp. 121–129.

[10] J. M. Kaye, F. P. J. Primiano, and D. N. Metaxas, "A three-dimensional virtual environment for modeling mechanical cardiopulmonary interactions," *Med. Image Anal.*, vol. 2, pp. 169–195, 1998.

[11] M. H. Tawhai and K. S. Burrowes, "Developing integrative computational models," *Anat. Rec.*, vol. 275B, pp. 207–218, 2003.

[12] H. Ding, Y. Jiang, M. Furmancyzk, A. Prkewas, and J. M. Reinhardt, "Simulation of human lung respiration using 3-D CFD with macro air sac system," presented at the Western Simulation Conf. Soc. Model. Simulation Int., New Orleans, LA, 2005.

[13] W. P. Segars, D. S. Lalush, and B. M. W. Tsui, "Modeling respiratory mechanics in the MCAT and the spline-based MCAT systems," *IEEE Trans. Nucl. Sci.*, vol. 48, no. 1, pp. 89–97, Feb. 2001.

[14] P. M. Sharkey, M. D. Ryan, and D. J. Roberts, "A local perception filter for distributed virtual environments," presented at the IEEE Virtual Reality Int. Symp., Atlanta, GA, 1998.

[15] F. G. Hamza-Lup, C. E. Hughes, and J. P. Rolland, "Distributed consistency maintenance scheme for interactive mixed reality environments," presented at the Int. Conf. Cybern. Inform. Technol. Syst. Appl., Orlando, FL, 2004.

[16] H. Fuchs, A. State, M. Livingston, W. Garrett, G. Hirota, M. Whitton, and E. D. Pisano, "Virtual environments technology to aid needle biopsies of the breast: An example of real-time data fusion," presented at the Medicine Meets Virtual Reality Conf., San Diego, CA, 1996.

[17] T. P. Caudell and D. W. Mizell, "Augmented reality: An application of heads-up display technology to manual manufacturing processes," in *Proc. 25th Hawaii Int. Conf. Syst. Sci.*, vol. 2, 1992, pp. 659–669.

[18] A. Webster, S. Feiner, B. MacIntyre, W. Massie, and T. Krueger, "Augmented reality in Architectural Construction, Inspection and Renovation," presented at the ASCE Third Congr. Comput. Civil Eng., Anaheim, CA, 1996.

[19] M. Billinghurst and H. Kato, "Collaborative augmented reality," *Commun. ACM*, vol. 45, pp. 64–70, 2002.

[20] R. Martins and J. P. Rolland, "Diffraction properties of phase conjugate material," in *Proc. SPIE*, vol. 5079, 2003, pp. 277–283.

[21] J. P. Rolland, L. D. Davis, and Y. Baillot, "A survey of tracking technology for virtual environments," in *Fundamentals of Wearable Computers and Augmented Reality*, W. Bardfield and Th. Caudell, Eds. Mahwah, NJ: Erlbaum, 2001, ch. 3, pp. 67–112.

[22] F. G. Hamza-Lup, L. Davis, C. E. Hughes, and J. P. Rolland, "Marker mapping techniques for augmented reality visualization," presented at the 17th Int. Symp. Comput. Inform. Sci., Orlando, FL, 2002.

[23] Y. Argotti, L. Davis, V. Outters, and J. P. Rolland, "Dynamic superimposition of synthetic objects on rigid and simple-deformable objects," *Comput. Graph.*, vol. 26, pp. 919–930, 2002.

[24] A. Santhanam, C. Fidopiastis, and J. P. Rolland, "An adaptive driver and real-time deformation algorithm for visualization of high-density lung models," in *Medical Meets Virtual Reality 12*. Newport, CA: IOS Press, 2004.

[25] A. Santhanam and J. P. Rolland, "An inverse deformation method for the visualization of 3D lung dynamics," (Abstract), presented at the Fourth Int. Conf. Ultrason. Imaging Tissue Elasticity, Austin, TX, 2005.

[26] A. Santhanam, C. Fidopiastis, K. Langen, S. Meeks, P. Kupelian, L. Davis, and J. P. Rolland, "Visualization of tumor-influenced 3D lung dynamics," *Proc. SPIE*, vol. 6141, pp. 61410C-1–61410C-12, 2006.

[27] A. MacRobert and T. Murray, "Spherical harmonics an elementary treatise on harmonic functions with applications," in *International Series of Monographs in Pure and Applied Mathematics*. New York: Pergamon, 1967.

[28] M. J. Ackerman, "The visible human project," *J. Biocommun.*, vol. 18, p. 14, 1991.

[29] F. G. Hamza-Lup and J. P. Rolland, "Adaptive scene synchronization for virtual and mixed reality environments," presented at the IEEE Virtual Reality Int. Symp., Chicago, IL, 2004.

[30] A. Santhanam, C. Fidopiastis, and J. P. Rolland, "A biomathematical model for pre-operative visualization of COPD and associated dyspnea," presented at the NIH Symp. Biocomput. Bioinform., Washington, DC, 2003.

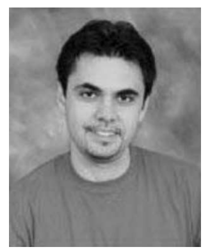

Felix G. Hamza-Lup received the B.Sc. degree in computer science from the Technical University of Cluj-Napoca, Cluj-Napoca, Romania, in 1999, and the M.S. and Ph.D. degrees in computer science from the University of Central Florida, Orlando, in 2001 and 2004, respectively.

Currently, he is an Assistant Professor of computer science at the School of Computing, Armstrong Atlantic State University, Savannah, GA. His current research interests include the development of novel human–computer interaction techniques based on augmented reality paradigms.

Dr. Hamza-Lup is a member of the Association for Computing Machinery (ACM) and Upsilon Pi Epsilon. He was the recipient of the Link Foundation Fellowship for advanced simulation and training and the Hillman Award for distinguished doctoral research in 2003.

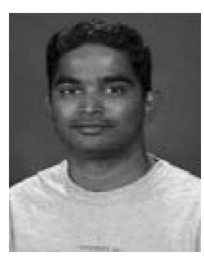

Anand P. Santhanam received the B.E. degree in computer science from the University of Madras, Chennai, India, and the M.S. degree in computer science from the University of Texas, Dallas, in 2001. He is currently working toward the Ph.D. degree at the School of Computer Science, University of Central Florida, Orlando.

His current research interests include real-time graphics and animation in virtual environments.

Mr. Santhanam was a recipient of the Link Foundation Fellowship from the University of Central Florida for advanced simulation and training.

Celina Imielińska received the M.E. degree in electrical engineering from the Politechnika Gdanska, Gdańsk, Poland, and the M.S. and Ph.D. degrees in computer science from Rutgers University, New Brunswick, NJ.

Currently, she is an Associate Research Scientist at the Department of Medical Informatics, College of Physicians and Surgeons, and the Department of Computer Science, Columbia University, New York, NY. Her current research interests include medical imaging, 3-D visualization, and computational geometry.

Sanford L. Meeks received the M.S. degree in physics from Florida State University, Tallahassee, in 1991, and the Ph.D. degree in medical physics from the University of Florida, Gainesville, in 1994.

He was an Associate Professor and Director of Radiation Physics at the University of Iowa. Currently, he is the Director of Radiation Physics at the M.D. Anderson Cancer Center, Orlando, FL. He is the coauthor of 15 book chapters and more than 50 peer-reviewed publications related to stereotactic radiosurgery, intensity-modulated radiation therapy, and image guidance.

Jannick P. Rolland received the Diploma from the Ecole Superieure D'Optique, Orsay, France, in 1984, and the Ph.D. degree in optical science from the University of Arizona, Tucson, in 1990.

Currently, she is an Associate Professor of optics, computer science, electrical engineering, and modeling and simulation at the University of Central Florida (UCF), Orlando.

Dr. Rolland was the receipient of the UCF Distinguished Professor of the Year Award in 2001 for the UCF Centers and Institutes and is a Fellow of the Optical Society of America (OSA). She is an Associate Editor of *Presence*. From 1999 to 2004, she was an Associate Editor of *Optical Engineering*.